Computational Fluid Dynamics Modeling of Ammonia Concen-Tration in a Commercial Broiler Building

João C. Gonçalves * , António M.G. Lopes , José L.S. Pereira

Posted Date: 19 April 2023

doi: 10.20944/preprints202304.0526.v1

Keywords: Ammonia emission; Broiler building; CFD; Measurement techniques; Outside climate

Article

Computational Fluid Dynamics Modeling of Ammonia Concentration in a Commercial Broiler Building

João C. Gonçalves [1,2,3,*], António M. G. Lopes [3] and José L. S. Pereira [1,4]

[1] Agrarian School of Viseu, Polytechnic Institute of Viseu, Quinta da Alagoa, 3500-606 Viseu, Portugal, jgoncalves@esav.ipv.pt;
[2] CERNAS-IPV Research Centre, Polytechnic Institute of Viseu, Campus Politécnico, Repeses, 3504-510 Viseu, Portugal
[3] ADAI-LAETA, Department of Mechanical Engineering, University of Coimbra, 3030-788 Coimbra, Portugal; antonio.gameiro@dem.uc.pt
[4] Centre for the Research and Technology of Agro-Environmental and Biological Sciences (CITAB), Inov4Agro, University of Trás-os-Montes and Alto Douro, Quinta de Prados, 5000-801 Vila Real, Portugal
* Correspondence: jgoncalves@esav.ipv.pt

Abstract: In the present study, a numerical model was developed to predict the flow pattern inside a broiler building. The model intends to predict the velocities fields inside the domain and ammonia (NH_3) emitted or released by litter from poultry housing. The numerical model developed in Computational Fluid Dynamics (CFD) commercial code, intends to represent a commercial broiler building, and intends to simulate the 3D and heat transfer, in steady state flow. The evaporative cooling pads were also included in the model. The validation of the model was based in experimental measurements obtained in previous studies. The simulations were focused on Summer, Winter and also Mid-Season situation. The numerical results of NH_3 concentration were compared with the experimental measurements, and a quite good agreement was verified. The numerical results allowed the characterization of: the inside flow pattern developed for the summer and winter situation; the inside NH_3 distribution, and the velocity field distribution inside the broiler building. It was found that NH_3 concentration increases along the tunnel, especially in low flow rate imposed from the exhaust fan. Also, it was verified that the low velocities inside domain are no sufficient to remove the gaseous pollutants.

Keywords: ammonia emission; broiler building; CFD; measurement techniques; outside climate

1. Introduction

The world population already exceeds seven billion people, is expected to exceed nine billion by 2050 and, at least, ten billion by the end of this century. The constant increase in the world population also leads to a need for increase in food production. Bird meat is a very important protein source for human consumption. World chicken meat production for 2022 is around 101 million tons worldwide [1]. The broiler production is highly developed and is oriented for two breeding goals: hens to obtain fertile eggs and broilers to obtain meat.

Ventilation of broiler buildings is very important as the decomposition of litter material in the floor generates manure and produces several harmful gases for humans and animals. Along with carbon dioxide (CO_2), the production of broiler also generates methane (CH_4) and nitrous oxide (N_2O), which are considered the main greenhouse gases, and pointed as one of the main causes of climate change, due to their potential contribution for global warming [2]. In face of the environmental problems caused by the gases emission in broiler production, international regulations have been published in order to reduce ammonia (NH_3) emissions, particularly the directive (European Union) 2016/2284 of 14 December, that aims a reduction in 20% of NH_3 emissions

 doi:10.20944/preprints202304.0526.v1

from animal housing by 2030 [3,4]. In addition, NH_3, N_2O and CH_4 contribute to acid rain, ozone formation in the troposphere and global warming [5].

Continuous exposure to high concentrations (> 15.2 mg/m^3 or > 20 ppm) of NH_3 is harmful to humans and animals [4,6], as it can cause several respiratory problems and eye irritation. Likewise, continuous exposure of broilers to this gas is reported to be the cause for reduction in the rate of weight gain and health problems [6,7]. In addition, international regulations also intend to protect birds and workers health, by limiting the exposure to NH_3. The volatilization of NH_3 is influenced by several factors such as temperature and relative humidity, ventilation rate and air velocity, excretion rate and litter removal schedule [6,8]. Some studies have been published concerning strategies to control and reduce NH_3 volatilization in broiler housing, either by adding additives to litter material or by dietary manipulation [2,5,9–14]. Strategies like the utilization of additives and the adoption of diets with lower levels of crude protein are some examples of measures that can contribute to reduce NH_3 losses in broiler production facilities [6].

Efficient ventilation strategies are of utmost importance for the healthy growth of broilers and low mortality rates. Additionally, productivity is highly dependent on indoor environmental conditions, since birds are very sensitive animals [15]. Broiler farms with inadequate ventilation systems can have high mortality rates when the air inside the building is hot, humid and nearly still in the microenvironment close to the broiler chickens. The uniformity of air velocity in the region occupied by the broilers is also important, to inhibit migration into better ventilated but already crowded areas, which also contributes to increased bird mortality [16]. The ventilation pattern used in broiler buildings is usually different from the cold to the warm season, and also depends on the stage of the fattening cycle of broiler production. Commercially, different typical ventilation patterns can be found, according to the number and location of the air exhaust ventilators and the outside air admission. For example, Fancom, The Netherlands, company can supply five different design configurations.

The inside thermal and dynamic parameters distribution that determines the internal climate like air temperature, velocity and relative humidity depends on several parameters such as: geometry and dimensions of the building, location and dimension of the air inlet and outlet, the ventilation regime, the envelope parameter's (walls, floor and ceiling) and, of course, outside conditions of temperature, relative humidity, wind and radiation. Typically, and most used in Portugal, the broiler buildings geometry consists in long tunnels equipped with extraction ventilators located in one extreme and on the top of the building. The outside air for refreshment enters through small openings on the lateral walls. These openings are automatic controlled and can open or close according to the external climatic conditions. The ventilation strategy is a compromise between the thermal comfort in terms of temperature and humidity, and the need to refresh the internal air and at the same time remove the gaseous pollutants.

Using appropriated methodology and equipment, experimental data may give important information about the air flow and other variables fields such as temperature and gases concentration. The main drawbacks of the experimental approach are the cost of equipment, the time needed to setup the measurement chain and perform the measurements and also the fact that it is only feasible to take measurements at a relatively reduced number of locations.

In the last years, numerical simulation tools have been improving, also benefiting from higher computer calculation and storage capabilities. The CFD techniques can be used to evaluate and optimize the buildings design to improve the thermal comfort in shopping's, state buildings as schools or hospitals, or in refrigerated food conservation equipment [17]. The CFD tools may be used to improve the indoor environment of livestock farms in terms of building design and farm operation. The CFD studies can be applied in existing broiler housing or before constructing the building. Therefore, the use of CFD techniques may contribute to reduce the cost of production and to increase the productivity of the animals [18]. In Rong et al., [19] the authors summarize the best practice guidelines for CFD modeling in livestock buildings to ensure prediction quality. Taking the advantages of CFD techniques, this methodology have been also used to simulate the indoor air flow on animal buildings, namely in pig housing [20,21], in cattle housing [22], and in particular in poultry

 doi:10.20944/preprints202304.0526.v1

housing [16,23]. In Eva Galdo (2017) [18], a review of animal buildings CFD simulations is presented. Of particular interest are the studies devoted to broiler buildings ([15,16,24–26]. The adequate design of broiler buildings, the location of inlet and exhaust air locations have been also investigated by several authors, such as [15,19,24,25].

The main objective of the present study is to develop a 3D CFD numerical model able to simulate the 3D fluid flow distribution inside a broiler building, in order to assess the indoor airflow pattern, and also gaseous pollutants concentration distribution like NH_3. We intend to characterize the field distribution NH_3 concentration and velocity inside the broiler building, for winter, mid-season and summer seasons. One important objective of the present study is to compare the NH_3 concentration, measured experimentally, in the real installations, with the numerical results. By comparing numerical and experimental results, an evaluation can be made on whether the locations of the gaseous collection selected sampling points in the experimental approach were sufficient and representative of the real distribution inside the building. In fact, by allowing the solution for the whole variables' fields, the CFD approach can provide a sound support to decide best location points for experimentally gas concentration sampling.

2. Material and Methods

2.1. Broiler Building

The building analyzed in the present work is one of the commercial broiler buildings studied in [3], in which the authors carried out an experimental work measuring the NH_3, N_2O, CO_2 and CH_4 concentration. The commercial broiler farm is located in Figueira da Foz, a small coastal town in center Portugal. The building is oriented in the East-West direction, has length 120 m, width 16 m, ridge 4.0 m and sidewall with height 2.7 m. The building has steel structure, a concrete floor and the side walls and ceiling are insulated with polyurethane. The building is equipped with 4 lines of automatic feeding systems, 4 lines of nipple drinking systems, evaporative cooling pads (model Celdek, Munters, Sweden). The climate control system is a model F37 from Fancom, The Netherlands.

The ventilation configuration consists of 5 roof exhaust fans, 8 exhaust fans at the top of the tunnel and 2 exhaust fans at the lateral walls near of the West top. The air inlet takes place through 52 small rectangular windows (0.38 m × 0.86 m) located in both lateral walls. The ventilation is made by minimum transitional tunnel ridge system being controlled with one differential pressure meter (0 – 100 Pa, Fancom, The Netherlands), two temperature sensors (SF7, Fancom, The Netherlands), and two relative humidity sensors (RHM.17 and a model RHO.17) indoors and outdoors.

2.2. Field Measurements

The experimental values used in the present study were those measure by [3]. These values will be used to assess the numerical method, by comparing the NH_3 concentration values measured at four different locations, and for 6 different situations (2 summer period, 2 winter period and 2 for mid-season period).

In [3], concentration values of NH_3, N_2O, CO_2 and CH_4 were measured indoors and outdoors in four different locations. The 4 indoor collecting points were located in the central part of the building along its main axis (x=14 m; x=23 m; x=50 m; x=77 m), at a distance of 0.5 m from the ground. Concentration measurements were monitored by a multipoint sampler connected to a photoacoustic field gas monitor (INNOVA 1409-12 and 1412i-5, Lumasense Technologies, Denmark). Air samples were collected in sequence through the sampling points, with gas concentration continuously measured and recorded every 2 minutes. For data comparison with the CFD model, hourly-averaged values are used. Table 1 lists the simulation conditions. More details about the experimental equipment and measurement procedures can be found in [3].

Preprints (www.preprints.org) | NOT PEER-REVIEWED | Posted: 19 April 2023 doi:10.20944/preprints202304.0526.v1

Table 1. Details of the configurations simulated in broiler building.

Configuration	Season	Correspondent Date	Grow period (day)	Hour of the day [h]	Broilers number	Liveweight [g]
W1	Winter	21/03/2018	31	6	37180	1141.0
W2	Winter	21/03/2018	31	14	37153	1170.0
S1	Summer	23/07/2018	28	6	36309	1214.1
S2	Summer	23/07/2018	28	14	36292	1245.0
MS1	Mid-season	07/10/2017	30	6	38718	1515.6
MS2	Mid-season	07/10/2017	30	14	38712	1533.0

3. CFD Model

3.1. Geometry, Numerical Model and Boundary Conditions

In this study, the commercial package ANSYS-CFX was used to create the numerical model for the simulations. The geometric model replicates the relevant features of the actual commercial broiler and may be seen in Figure 1. The air inlet is done through 52 windows with dimensions 0,38 m × 0,86 m, 26 windows located in each of the lateral walls. The exhaust is done by 5 fans placed at the ceiling, 8 fans at the top west and 2 fans at each lateral wall near the top of the tunnel. Due to their small size in comparison with the building dimensions, the feeding and drinking lines, the measurement equipment as well as other obstacles, were not taken in account in the simulations.

The lateral walls and the ceiling were considered as adiabatic. At the floor, a heat flux rate was imposed to simulate the metabolic heat release rate of the broilers and also from the litter. [27] conclude that the total heat production - THP (sum of sensible and latent bird heat production) depends on the broilers growing cycle day, inner temperature, day period (light and dark) and birds' weight. For the present case and according to the methodology proposed by these authors, a total specific heat release rate of 8 W/kg and 10 W/kg was adopted for summer and for the winter situations, respectively. The NH_3 release rate from the litter was also considered in the simulations made in this study. Considering the experimental results of Pereira et al. (2018) [3], the values listed in Table 2 were used. The broiler building was equipped with evaporative cooling pads 21.0 × 1.8 m (model Celdek 7060-15, Munters, Sweden) and 100 mm thickness, installed along the lateral walls (Figure 1). The evaporative pads, parallelepipedal in shape, were simulated as a porous medium, with corresponding properties calculated following the methodology reported in [28] and also used in the work of [29].

The flow inside the broiler building is considered as steady state, incompressible and turbulent. Due to symmetry conditions relative to the longitudinal vertical plane located at mid-width, only half of the domain was simulated. [30] evaluated several turbulence models for assessing the indoor environment of a broiler building and concluded that the RNG k–ε model showed the best agreement with the measurements of velocity and temperature. This model was thus adopted for the present simulations. The governing equations were discretized using the high resolution and the upwind schemes for the convective and for the turbulent terms, respectively. The iterative calculation procedure was assumed close enough to the convergence when all residuals became lower than 10^{-4}.

Table 2. Boundary and initial conditions of the simulated configurations in broiler building.

Configuration	T_{int} [ºC]	Hr_{int} [%]	T_{out} [ºC]	Hr_{out} [%]	Outlet volume flow rate [m³/h]	Outlet mass flow rate [kg/s]	NH_3 Litter emission [kg/(m².s)]	Broiler Heat Released [W/m²]
W1	24.0	61.6	6.0	65.4	46300.3	16.0	2.87E-08	220.95
W2	25.3	59.0	13.2	54.7	72906.9	22.0	3.44E-08	226.40

Preprints (www.preprints.org) | NOT PEER-REVIEWED | Posted: 19 April 2023 doi:10.20944/preprints202304.0526.v1

S1	26.1	80.9	19.6	88.2	90620.5	30.2	9.40E-08	344.39
S2	29.1	62.7	25.9	55.5	210754.2	70.3	1.86E-07	353.00
MS1	24.7	73.4	9.5	94.3	115777.4	39.1	6.99E-08	305.06
MS2	30.4	39.2	28.7	26.9	300510.0	100.7	1.90E-07	309.09

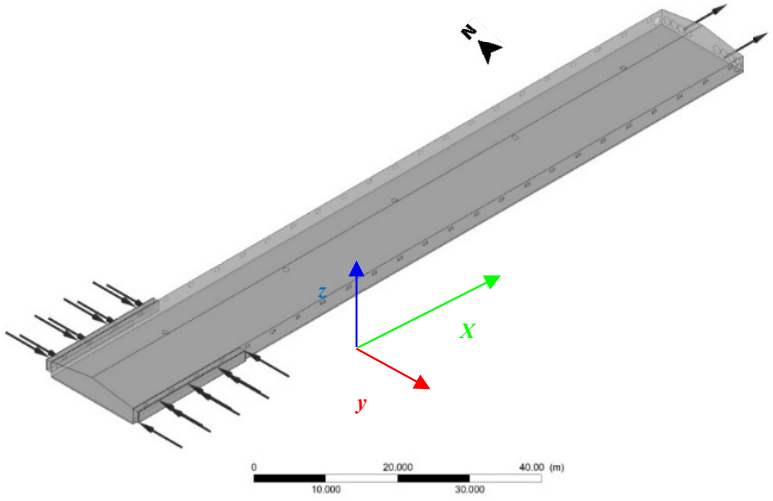

Figure 1. Geometry domain representative of the broiler building, with the inlet fresh air in the evaporative pad (lower left corner of the Figure), and the outlet at the end of the tunnel.

3.2. Conditions or Configurations Simulated and Boundary Conditions

Six different situations were simulated to replicate summer, winter, and mid-season conditions, including the day and night periods. All the conditions correspond to the final stage of the broilers growing cycle, that lasts approximately 30 days. Table 1 and Table 2 summarizes all the conditions of the simulated configurations in the broiler building.

3.3. Mesh Independence Tests

Besides other factors, results from the CFD simulations can be greatly affected by mesh design and refinement. To keep discretization errors as low as possible, higher nodes concentration should be ensured in regions of large spatial variations. For that purpose, the mesh was refined near solid boundaries and at inlets and outlets.

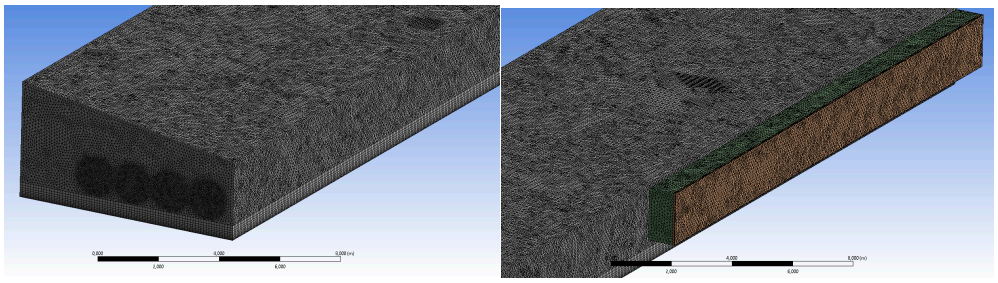

Figure 2. Details of the mesh, showing the mesh refinement at the outlet and inlet surfaces, in the litter and in the Evaporative pad of the broiler building.

To evaluate mesh independence, four meshes with different sizes were created and the simulation results compared. Table 4 presents the number of elements and nodes of the tested meshes.

Preprints (www.preprints.org) | NOT PEER-REVIEWED | Posted: 19 April 2023 doi:10.20944/preprints202304.0526.v1

Table 3. Mesh details of the broiler building.

	Nº nodes	Nº Elements
Mesh 1	479973	1656020
Mesh 2	608814	2343413
Mesh 3	1222894	5478648
Mesh 4	2241341	10581101

Mesh dependency analysis was made based on the average value of NH_3 volume fraction values at the global Outlet Surface and in a horizontal plane at height z=0.2 m, for the 4 different mesh tested. Figure 3 shows the results for all the four meshes.

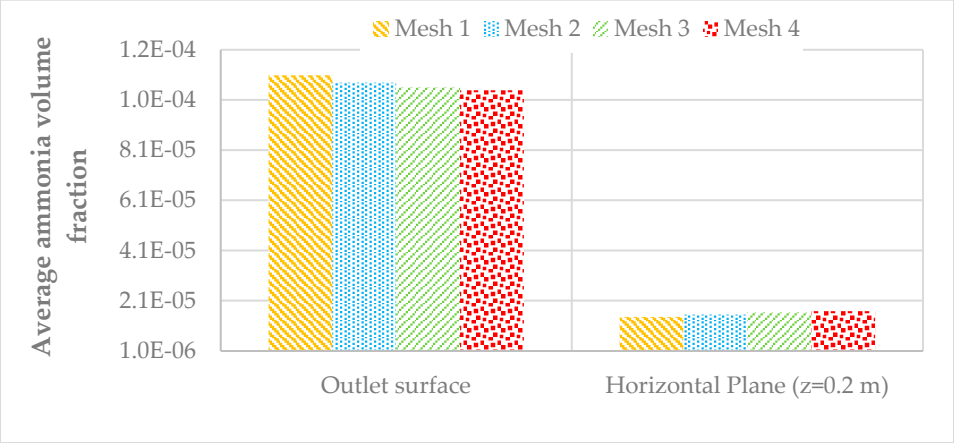

Figure 3. Average NH_3 volume fraction values at the global Outlet Surface and at *z*=0.2 m plane, for the 4 tested meshes of the broiler building.

Once results for Mesh 3 and 4 were close enough, in order to optimize the time computer calculation effort and the CFD accurate results, Mesh 3 was considered in all further simulations.

4. Results and Discussion

4.1. Comparison of Experimental and Numerical Results for NH_3 Concentration

As previously referred, the main motivation and objective of the present study is to simulate the airflow inside a broiler building and to verify the model results by comparing the obtained NH_3 concentration with the experimental measurements. For this propose, a simulation campaign was carried for the conditions presented in Table 2.

For the experimental results, average values were computed from measurements at 4 collecting points located in the central part of the building along the tunnel main axis at locations x=14 m; x=23 m; x=50 m; x=77 m, at a height 0.5 m from the ground [3]. Figure 4 compares the experimental and numerical average values of NH_3 concentration for the different simulated configurations. Globally, a quite good agreement is obtained between numerical and experimental results. The best agreement is obtained for configuration Winter 2 (W2) and Midseason 2 (MS2), with almost coincident results. On the opposite, the largest difference was verified for configurations Winter 1 (W1) and Summer 1 (S1), with CFD NH_3 concentration underestimations of 36% and 17%, respectively.

The midseason configurations MS1 and MS2 have the two largest number of, leading to a larger NH_3 generation. In spite of this, largest NH_3 concentrations are obtained, both numerically and experimentally, for the two Summer configurations, S1 and S2. This is most likely because in the midseason configurations ventilation rates are higher and pollutants are thus removed more effectively.

Preprints (www.preprints.org) | NOT PEER-REVIEWED | Posted: 19 April 2023 doi:10.20944/preprints202304.0526.v1

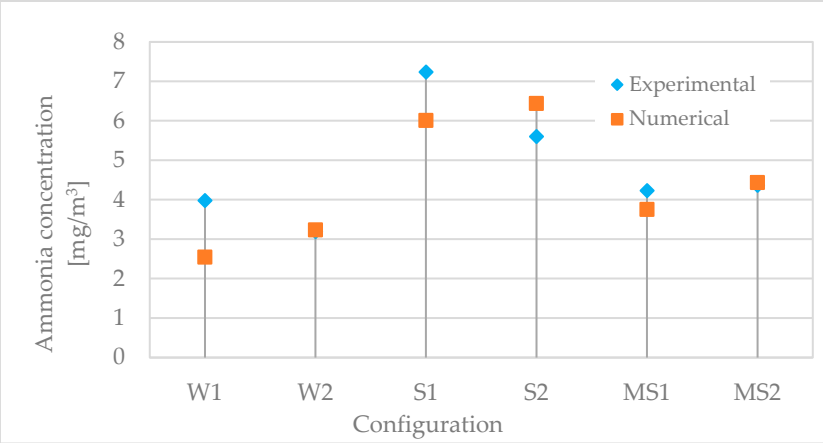

Figure 4. Experimental and Numerical average values of NH_3 concentration from 4 collecting points, and for the different configuration simulated in the broiler building.

4.2. Characterization of Indoor Air Flow for Different Configurations

Airflow pattern

As referred in section 3.2, six different situations were simulated to replicate summer, winter, and mid-season conditions, as listed in Table 2. Numerical simulations show that the flow pattern inside the broiler building is quite complex and very much dependent on the thermal and dynamic initial conditions. This can be observed in Figure 5, that shows the streamlines for S1 and MS2 configurations, with representation at half domain. For the S1 configuration, the flow pattern along the longitudinal direction (x-axis) is characterized by the formation of strong vortices immediately after the air enters in the domain, as clearly shown in Figure 5(a). This pattern is also observed in MS1 configuration, and is even more intense for the winter configuration. The consequence is a significant variation of the local properties inside the domain for different initial conditions.

A different flow pattern is observed in the MS2 configuration (Figure 5(b)). For this configuration, although in the initial zone of the air inlet the flow pattern is similar to that verified in S1, the longitudinal vortices of configuration S1 are not verified but, instead, the streamlines become linear and parallel to each other. This different behavior is due to the higher exhaust air flow rates imposed in the initial conditions. Thus, in this configuration, the inertial forces are larger than the viscous forces and turbulence almost disappears. In these cases, and at least for zones far away from the inlet, the flow is clearly characterized as a displacement flow, with higher predictability of local flow properties. This airflow pattern also promotes a better and effective removal of pollutants presented in the compartment. However, as a disadvantage, the higher flow velocity may cause discomfort. This will be confirmed in further figures showing NH_3 concentration and velocity profiles.

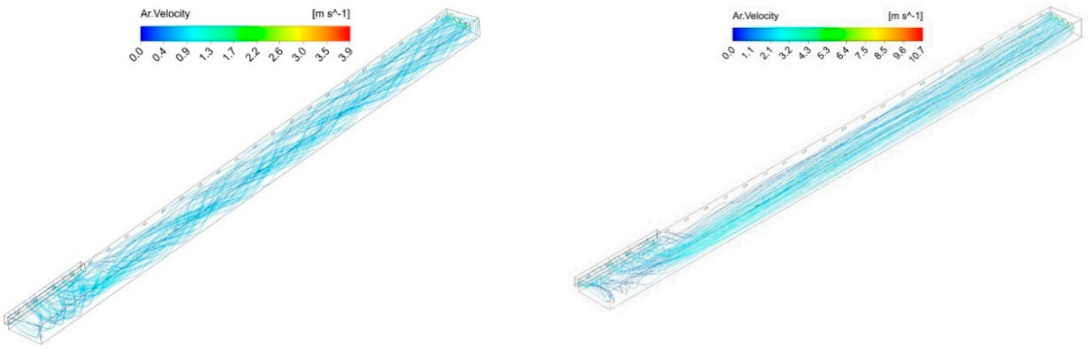

(a) S1 (b) MS2

Figure 5. Streamlines for two configurations in the broiler building.

Preprints (www.preprints.org) | NOT PEER-REVIEWED | Posted: 19 April 2023 doi:10.20944/preprints202304.0526.v1

Figure 6 shows the velocity vectors in a vertical plane located at x=15 m, for configurations S1 and MS2. This Figure clearly confirms the flow complexity and the differences between these two configurations, with configuration MS2 showing two large vortices rotating in opposite directions. In configuration S1, the lower air temperature at the inlet forces the flow down, creating a single large vortex that proceeds downstream as seem in Figure 5(a). In configuration MS2, the higher values of temperature and inlet air velocity originate a different flow pattern. In this case, two opposite recirculation cells are observed. This behavior is obviously strongly dependent of inlet and initial conditions, which, once again, originate the great local variability of the properties. So, special attention must be dedicated in the selection of the location of sample collection points in field measurements.

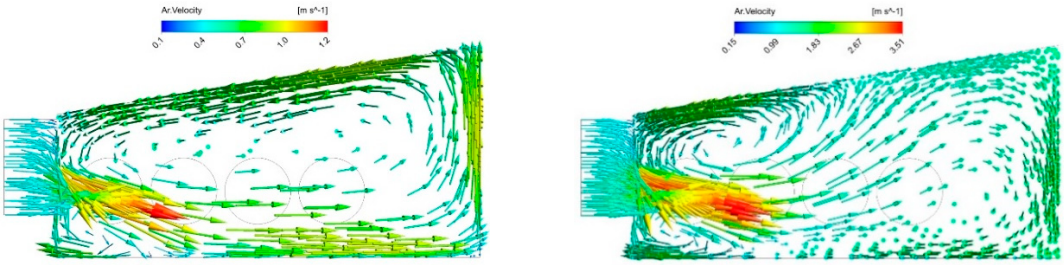

(a) S1 (b) MS2

Figure 6. Vector profile in a plane yz, and at x=15 m, for the configurations: (a) S1, and (b) MS2 in the broiler building.

Ammonia distribution

Figure 7 shows the NH_3 volume fraction distribution in a horizontal plane located at z = 0.5 m from ground, for the 6 simulated configurations. As expected, concentration values increase from the inlet zone to the exhaust zone, as the fresh air entering the domain through the evaporative pad is contaminated by NH_3 released from the ground (i.e., litter material).

Mid-Season configurations are characterized by a significant exhaust ventilation rate, so the NH_3 is more effectively removed as can be observed in Figure 7(d). This configuration is characterized by the tunnel (displacement) ventilation, with parallel streamlines along the tunnel. In the MS2 configuration, the NH_3 emission is similar to the S2 configuration; however, in MS2 the ventilation rate is 50% larger than in S2 configuration.

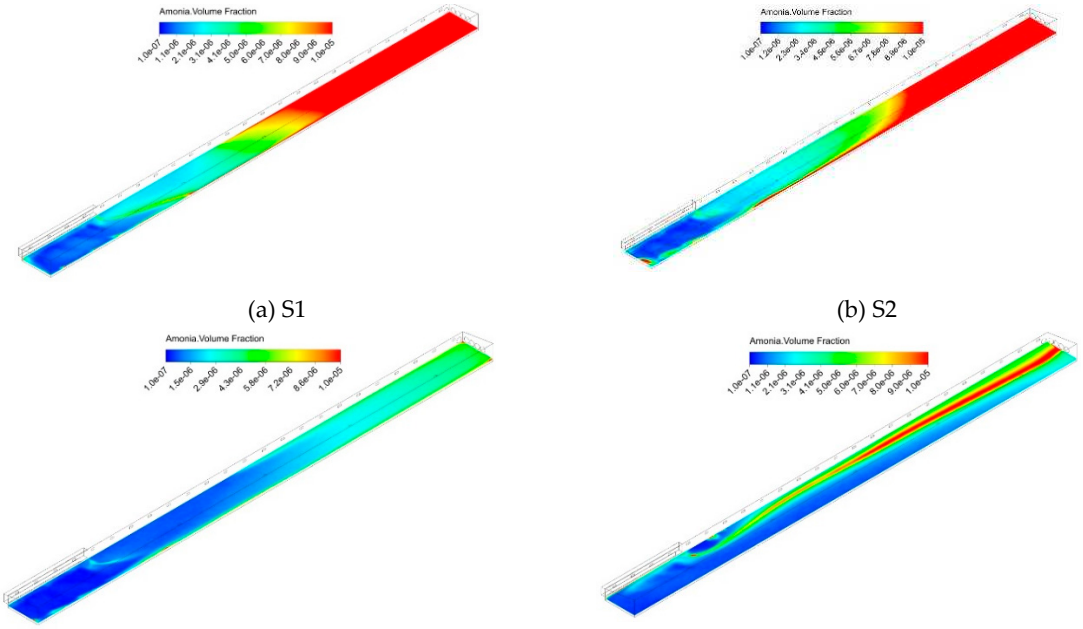

(a) S1 (b) S2

(c) MS1 (d) MS2

Preprints (www.preprints.org) | NOT PEER-REVIEWED | Posted: 19 April 2023 doi:10.20944/preprints202304.0526.v1

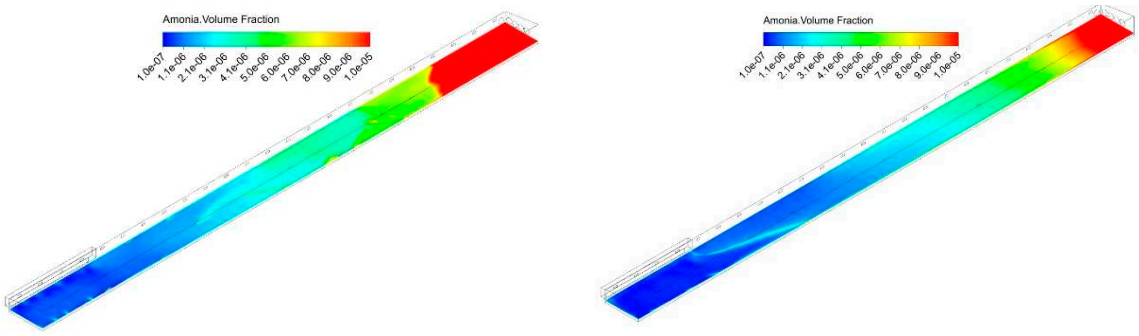

(e) W1 (f) W2

Figure 7. Color contours of NH_3 concentration (volume fraction) in a plane at z = 0.5 m from ground, for the 6 configurations simulated in the broiler building.

In Winter situations the outside air temperature, as well as, the exhaust ventilation rate is significant lower. Figure 7(e) and (f) shows the contours of NH_3 concentration for these situations. Although in Winter situation the flow velocities are much lower, we can confirm that, just as in configurations S1 and S2, also in configurations W1 and W2 the NH_3 concentration increases in a considerable amount near the exhaust zones, at the tunnel exit. This also indicates that the exhaust flow rate imposed by the fans is not sufficient to efficiently remove the NH_3.

To better understand the NH_3 distribution, this property was averaged in the transversal y direction using 15 sampling points and plotted in Figure 8 as function of the longitudinal x direction at height z=0.5 m and z=1.8 m. Although the vertical scale of the graph is limited to 30 mg/m³ for better depicting the evolution of NH_3 concentration in the first half of the tunnel, NH_3 concentration reaches values larger than 40 mg/m³ for configurations S1, S2, and W1.

From the Figure 7 it may be concluded that NH_3 is efficiently removed from the building in configurations MS1, MS2 and W2. On the opposite, in configuration S1, S2, and W1 the NH_3 concentration substantially increases after the mid-length of the tunnel. It may be also noticed in Figure 8 (a) and (b) that the NH_3 concentration distribution is rather similar at heights of z=0.5 m and z=1.8 m. Previous studies [3,4,6] recommend a limit of 7.6 mg/m³ (10 ppm) of NH_3 to maintain a good indoor air quality on broiler buildings, but the threshold values of 15.2 mg/m³ (20 ppm) are recommended as limit for a short period exposure. Note that long-term NH_3 toxicity in the broiler building may increase the susceptibility of birds to the adverse effects of NH_3 even at 15.2 mg/m³ [4,6].

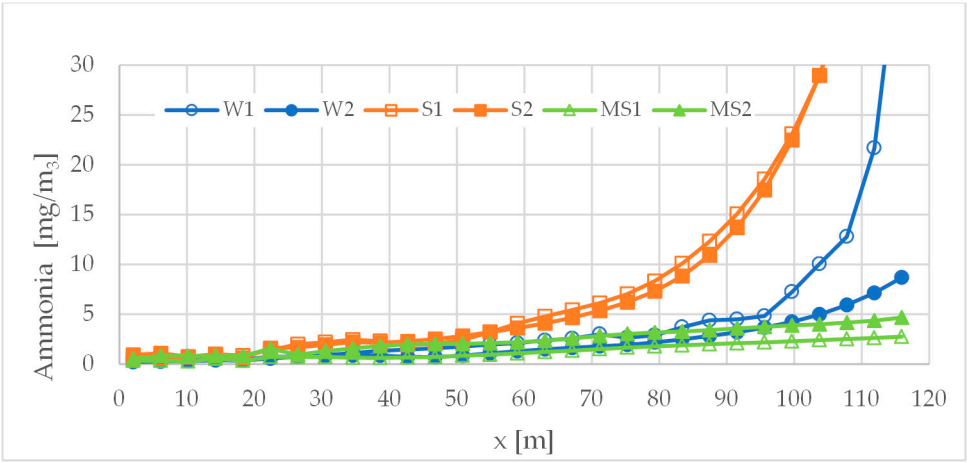

(a)

Preprints (www.preprints.org) | NOT PEER-REVIEWED | Posted: 19 April 2023 doi:10.20944/preprints202304.0526.v1

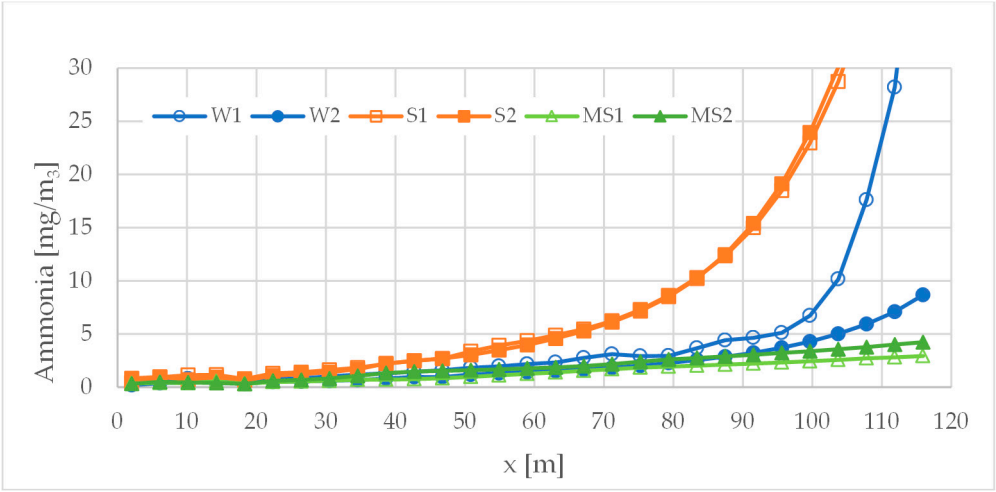

(b)

Figure 8. Average NH_3 concentration at each x location at height (a) z=0.5 m and (b) z=1.8 m in the broiler building.

Figure 9 represents the NH_3 concentration along the longitudinal x direction at y = 7.5 m, at constants heights from the ground z=0.5 m and z=1.8 m. Comparing these local concentration values obtained at a specific y transversal location with the concentration values averages over the transversal direction depicted in Figure 8, it may be noted that, at least up to x=60 m, the local concentration values (Figure 9(a)) are always higher. Thus, despite of the same trend observed, it may be concluded that the experimental point measurement methodology are, in this case, overestimating the values of gas concentration.

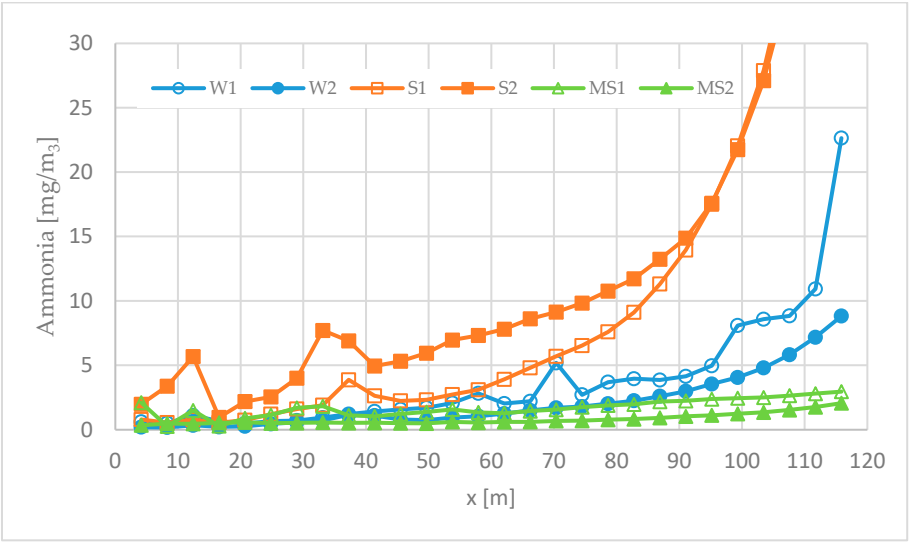

(a)

Preprints (www.preprints.org) | NOT PEER-REVIEWED | Posted: 19 April 2023 doi:10.20944/preprints202304.0526.v1

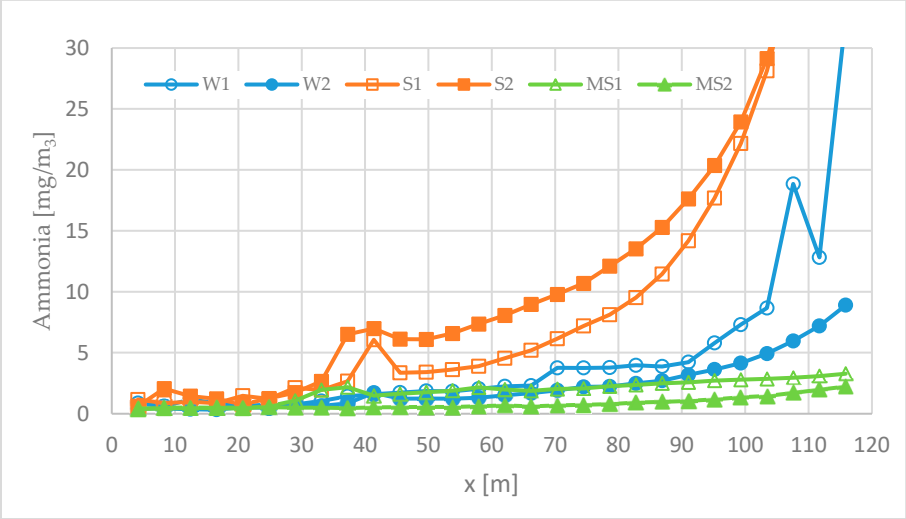

(b)

Figure 9. Ammonia concentration profile along the tunnel in a line (x direction), located at y=7.5 m and at high of: (a) z=0.5 m and (b) z=1.8 m in the broiler building.

We can also underline that, taking into account the numerical results, it is verified that the NH_3 concentration at the outlets is much higher than the average values obtained in the longitudinal line, the average in the horizontal plane (cf. Figures 8), and also the values measured experimentally at the 4 sample collection points (cf. Figure 3). Thus, it is predicted that the methods that consist in collecting the gases at the outlet may overestimate the average concentration inside the building.

Velocity distribution

Figure 10 shows the velocity distribution colored with the local air velocity values, for all the configurations. Are also printed the average velocity values at z=0.5 m. Not surprisingly, the highest values of indoor air velocity are verified in configurations MS2 and S2, because these were also the configurations where the highest exhaust ventilation rates imposed in the numerical calculation. Particularly in MS2 configuration, there is a large central extension where velocity exceeds 2 m/s. The same occurs in configuration S2, but only in the area in front of the air inlets. The highest velocity values are observed at the outlet surface (exhaust fans). These high velocity areas are prone to cause more stress to the broilers. However, we must underline that these situations refer to the final stage of the growing period (day 30), characterize by low mortality rate, due to the greater broilers' resistance. The opposite is verified for the winter configurations, and also for S1, with zones where the velocity doesn't reach 1 m/s, representing difficulties for the removal of gaseous pollutants, in particular NH_3, as verified in Figures 7 and 8.

For configurations W1 and W2, as the exhaust air flow rate are lower, the inner air velocities are also lower, with average velocity values 0.35 m/s and 0.49 m/s in plane z=0.5 m, for W1 and W2 configurations, respectively. In these configurations, as the inner air velocities are lower, it is verified that buoyancy forces are significant, overlapping the inertial forces of the longitudinal flow, which causes an increase in NH_3 concentration along the tunnel (cf. Figure 9).

It can also be identified, in all situations, the existence of a recirculation and almost stagnation zone, near the lateral wall and immediately after the air intake, approximately between x=20 m and x=30 m.

Preprints (www.preprints.org) | NOT PEER-REVIEWED | Posted: 19 April 2023 doi:10.20944/preprints202304.0526.v1

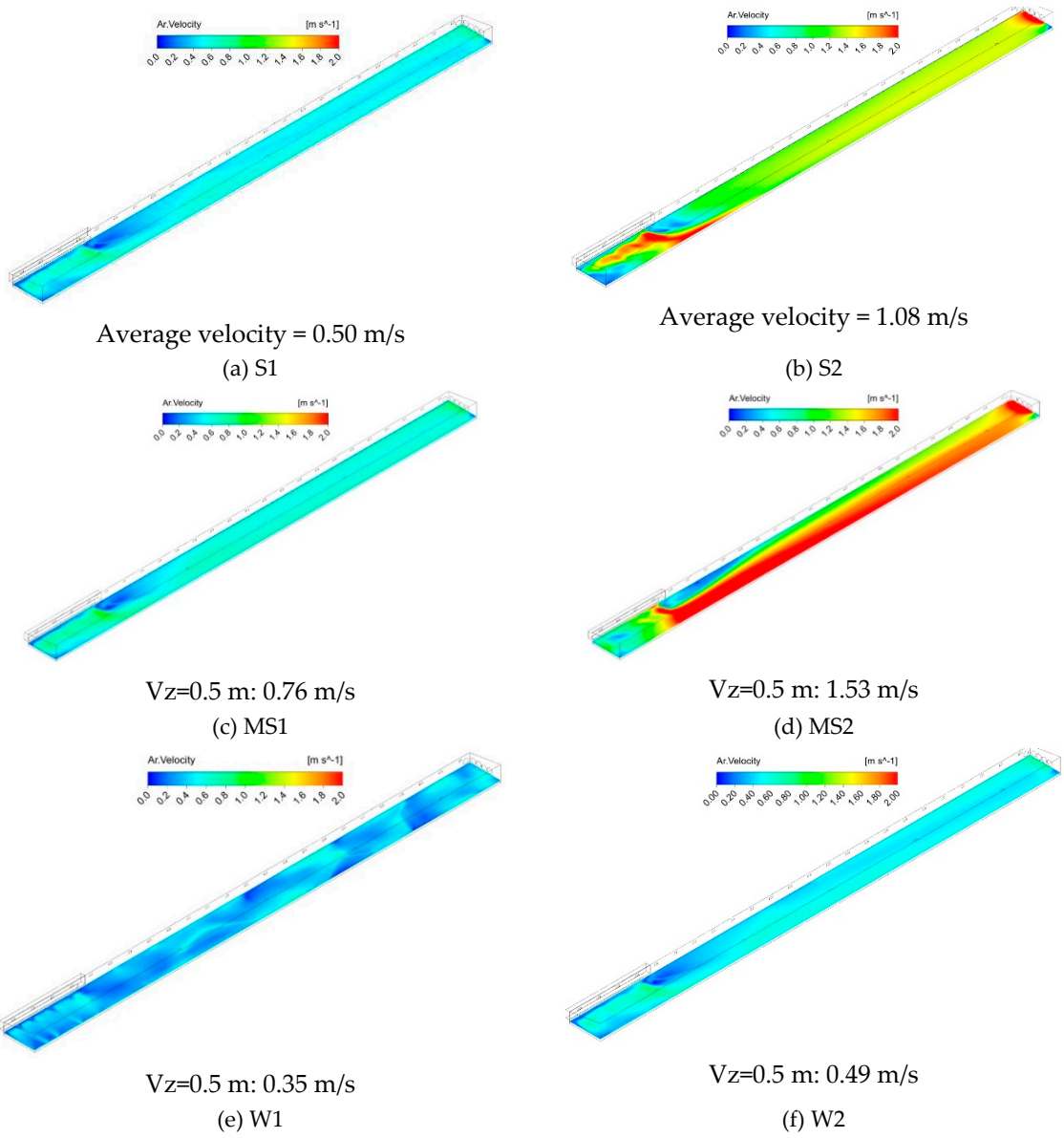

Figure 10. Horizontal plane at z=0.5 m, colored with the local velocity for the 6 simulated configurations in the broiler building.

Cited by [15], [31] reported that the optimum air velocity in individual boiler building should be in the range between 1.5 m/s and 2 m/s. In the present, numerical results identify several zones where air velocity is lower than 1 m/s, observed particularly in the Winter configurations, and higher than 2 m/s observed in MS2 configuration (cf. Figure 10).

5. Conclusions

In this study a 3D numerical model was developed to predict the flow field pattern inside a broiler building. Six different configurations were explored, corresponding to Summer, Winter and Mid-Season situations, for which experimental data was available. The numerical simulations considered all available experimental data, both geometrical and dynamic, used as initial and boundary conditions.

The experimental results of the average NH_3 concentration obtained at four sampling points for the six explored configurations were compared with the numerical results, and, globally, a quite good agreement between the results from both experimental and numerical methodologies was verified.

The results of numerical simulations, namely through streamlines, show that the flow pattern inside the broiler building is quite complex, and very dependent on the thermal and dynamic initial

conditions. This complexity is justified by the geometrical configuration, namely the positions of the of the air inlet and outlet, and by the confrontation of the inertia forces of the flow and the thermal buoyancy forces.

The flow complexity and large local variation of properties reenforce the special attention needed in the choice of the location of sample collection points in field experimental measurements, to better evaluate the property values represent their value of the entire domain, which is one of the important contributions of the paper.

The numerical model allowed the calculation of the NH_3 distribution in all the domain. Depending on the configuration, gaseous pollutants such as NH_3 may or may not be removed efficiently. It was found that in winter and summer configurations, in which the extraction flow rate was lower, the NH_3 concentration increased considerably along the tunnel, with no efficient removal of NH_3. On the other hand, in situations where the air extraction flow rates were high (mid-season), the NH_3 was efficiently removed, maintaining low concentrations throughout the tunnel.

Finally, concerning to the velocity field, the numerical simulations allowed to o identify configurations where the indoor air velocity is lower than recommended, namely in winter but also in summer situations. In fact, in configurations W1, W2 and S1, in which the extraction flow rates were lower, it can be observed that, at the level slightly above the birds z=0.5 m, there are zones where the air velocity is less than 1 m/s. This justifies also the difficulty verified in the removal of NH_3 in these configurations. In addition, the selection of indoor sampling points should be made carefully for a precise assessment of the gas indoor concentration.

Funding: This work is supported by National Funds by FCT - Portuguese Foundation for Science and Technology, under the project UIDB/04033/2020.

Acknowledgment: This work is supported by National Funds by FCT - Portuguese Foundation for Science and Technology, under the project UIDB/04033/2020; and also, FCT-Foundation for Science and Technology, I.P., within the scope of the projects Refª UIDB/00681/2020. Furthermore, we would like to thank the CERNAS Research Centre and the Polytechnic Institute of Viseu for their support.

References

1. USAD of Agriculture. Livestock and Poultry: World Markets and Trade. USDA Foreign Agricultural Service 2022. https://www.fas.usda.gov/data/livestock-and-poultry-world-markets-and-trade (accessed September 15, 2022).
2. Anderson K, Moore PA, Martin J, Ashworth AJ. Evaluation of a Novel Poultry Litter Amendment on Greenhouse Gas Emissions. Atmosphere 2021;12:563. https://doi.org/10.3390/atmos12050563.
3. Pereira JLS, Ferreira S, Pinheiro V, Trindade H. Ammonia, Nitrous Oxide, Carbon Dioxide and Methane Emissions from Commercial Broiler Houses in Mediterranean Portugal. Water Air Soil Pollut 2018;229:377. https://doi.org/10.1007/s11270-018-4026-4.
4. S N, Aj K. Ammonia production in poultry houses can affect health of humans, birds, and the environment-techniques for its reduction during poultry production. Environmental Science and Pollution Research International 2018;25. https://doi.org/10.1007/s11356-018-2018-y.
5. Bittman S, Sheppard SC, Hunt D. Potential for mitigating atmospheric ammonia in Canada. Soil Use and Management 2017;33:263–75. https://doi.org/10.1111/sum.12336.
6. Oliveira MD, Sousa FC, Saraz JO, Calderano AA, Tinôco IFF, Carneiro APS. Ammonia Emission in Poultry Facilities: A Review for Tropical Climate Areas. Atmosphere 2021;12:1091. https://doi.org/10.3390/atmos12091091.
7. Berry Lott. Amônia. Avicultura Industrial 2016. https://www.aviculturaindustrial.com.br/imprensa/amonia/20030711-113203-0098 (accessed September 15, 2022).
8. Broucek J. Nitrous Oxide Release from Poultry and Pig Housing. Polish Journal of Environmental Studies 2018;27. https://doi.org/10.15244/pjoes/75871.
9. Anderson Kelsey, Moore Philip Jr. A., Martin Jerry, Ashworth Amanda. Effect of a new manure amendment on ammonia emissions from poultry litter. Atmosphere 2020;257:1–14. https://doi.org/10.3390/atmos11030257.

10. Inoue KRA, Tinôco I de FF, Cassuce DC, Bueno MM, Graña AL. ANÁLISE DA CONCENTRAÇÃO DE AMÔNIA EM GALPÕES DE FRANGO DE CORTE SUBMETIDOS A DIFERENTES DIETAS. Revista Engenharia na Agricultura - REVENG 2012;20:19–24. https://doi.org/10.13083/reveng.v20i1.199.
11. Khan DR, Wecke C, Liebert F. An Elevated Dietary Cysteine to Methionine Ratio Does Not Impact on Dietary Methionine Efficiency and the Derived Optimal Methionine to Lysine Ratio in Diets for Meat Type Chicken. Open Journal of Animal Sciences 2015;5:457–66. https://doi.org/10.4236/ojas.2015.54047.
12. Medeiros R, Santos BJM, Freitas M, Silva OA, Alves FF, Ferreira E. A adição de diferentes produtos químicos e o efeito da umidade na volatilização de amônia em cama de frango. Cienc Rural 2008;38:2321–6. https://doi.org/10.1590/S0103-84782008000800035.
13. Moore P. Methods of treating manure. Patents Granted 2006.
14. Vilela M de O, Gates RS, Souza C de F, Junior CG de ST, Sousa FC. Nitrogen transformation stages into ammonia in broiler production: sources, deposition, transformation and emission to environment. DYNA 2020;87:221–8. https://doi.org/10.15446/dyna.v87n214.83318.
15. Küçüktopcu E, Cemek B, Simsek H, Ni J-Q. Computational Fluid Dynamics Modeling of a Broiler House Microclimate in Summer and Winter. Animals 2022;12:867. https://doi.org/10.3390/ani12070867.
16. Blanes-Vidal V, Guijarro E, Balasch S, Torres AG. Application of computational fluid dynamics to the prediction of airflow in a mechanically ventilated commercial poultry building. Biosystems Engineering 2008;100:105–16. https://doi.org/10.1016/j.biosystemseng.2008.02.004.
17. Gonçalves JC, Costa JJ, Figueiredo AR, Lopes AMG. CFD modelling of aerodynamic sealing by vertical and horizontal air curtains. Energy and Buildings 2012;52:153–60. https://doi.org/10.1016/j.enbuild.2012.06.007.
18. Eva Hilda Guerra Galdo. Evaluación de alternativas en las instalaciones avícolas de pollos de carne para la mejora de las condiciones de confort de los animales. Instituto de Ciencia y Tecnología Animal, Universitat Politècnica de València, 2017.
19. Rong L, Nielsen PV, Bjerg B, Zhang G. Summary of best guidelines and validation of CFD modeling in livestock buildings to ensure prediction quality. Computers and Electronics in Agriculture 2016;121:180–90. https://doi.org/10.1016/j.compag.2015.12.005.
20. Iqbal A, Gautam KR, Zhang G, Rong L. Modelling of animal occupied zones in CFD. Biosystems Engineering 2021;204:181–97. https://doi.org/10.1016/j.biosystemseng.2021.01.022.
21. Shin H, Kwak Y, Jo S-K, Kim S-H, Huh J-H. Applicability evaluation of a demand-controlled ventilation system in livestock. Computers and Electronics in Agriculture 2022;196:106907. https://doi.org/10.1016/j.compag.2022.106907.
22. Pakari A, Ghani S. Comparison of different mechanical ventilation systems for dairy cow barns: CFD simulations and field measurements. Computers and Electronics in Agriculture 2021;186:106207. https://doi.org/10.1016/j.compag.2021.106207.
23. Tong X, Zhao L, Heber AJ, Ni J-Q. Development of a farm-scale, quasi-mechanistic model to estimate ammonia emissions from commercial manure-belt layer houses. Biosystems Engineering 2020;196:67–87. https://doi.org/10.1016/j.biosystemseng.2020.05.008.
24. Li H, Rong L, Zong C, Zhang G. A numerical study on forced convective heat transfer of a chicken (model) in horizontal airflow. Biosystems Engineering 2016;150:151–9. https://doi.org/10.1016/j.biosystemseng.2016.08.005.
25. Li J, Suvarna M, Li L, Pan L, Pérez-Ramírez J, Ok YS, et al. A review of computational modeling techniques for wet waste valorization: Research trends and future perspectives. Journal of Cleaner Production 2022;367:133025. https://doi.org/10.1016/j.jclepro.2022.133025.
26. Osorio Hernandez R, Tinôco I, Mendes L, Guerra Garcia L, Barbari M, Baptista F, et al. CFD modeling of the thermal environment in a negative pressure tunnel ventilated broiler barn during the first week of life. 2015.
27. Chepete HJ, Xin H. Heat and Moisture Production of Poultry and Their Housing Systems: Pullets and Layers. ASHRAE Transactions 2004:15.
28. Franco A, Valera DL, Peña A, Pérez AM. Aerodynamic analysis and CFD simulation of several cellulose evaporative cooling pads used in Mediterranean greenhouses. Computers and Electronics in Agriculture 2011;76:218–30. https://doi.org/10.1016/j.compag.2011.01.019.
29. Fidaros D, Baxevanou C, Bartzanas T, Kittas C. Numerical study of mechanically ventilated broiler house equipped with evaporative pads. Computers and Electronics in Agriculture 2018;149:101–9. https://doi.org/10.1016/j.compag.2017.10.016.

30. Küçüktopcu E, Cemek B. Evaluating the influence of turbulence models used in computational fluid dynamics for the prediction of airflows inside poultry houses. Biosystems Engineering 2019;183:1–12. https://doi.org/10.1016/j.biosystemseng.2019.04.009.
31. Yahav S, Straschnow A, Vax E, Razpakovski V, Shinder D. Air Velocity Alters Broiler Performance Under Harsh Environmental Conditions1. Poultry Science 2001;80:724–6. https://doi.org/10.1093/ps/80.6.724.